Water Vapor Continuum Absorption in the Microwave

Vivienne H. Payne, Eli J. Mlawer, Karen E. Cady-Pereira, and Jean-Luc Moncet

***Abstract*—The accurate modeling of continuum absorption is crucial for the so-called window regions of the spectrum, the relatively transparent regions between lines. The window regions in the microwave are of critical importance for Earth remote sensing and data assimilation. Presented in this paper is an evaluation of the widely used Mlawer, Tobin, Clough, Kneizys, and Davis (MT_CKD) water vapor continuum model in the microwave region, performed using measurements from ground-based radiometers operated by the Department of Energy's Atmospheric Radiation Measurement Program at sites in Oklahoma, USA, and the Black Forest, Germany. The radiometers used were the Radiometrics 23.8/31.4-GHz microwave radiometers (MWRs), the Radiometer Physics GmbH 90/150-GHz MWR at high frequencies (MWRHF), and the Radiometrics 183 GHz G-band vapor radiometer profiler (GVRP). Radiometer measurements were compared with brightness temperatures calculated using radiosonde temperature and humidity profiles input to the monochromatic radiative transfer model (MonoRTM), which uses the MT_CKD continuum model. Measurements at 23.8 GHz were used to correct for biases in the total precipitable water vapor (PWV) from the radiosondes. The long-term 31.4 GHz data set, with a range of PWV values spanning from 0.15 to 5 cm, allowed the separation of uncertainties in the self- and foreign-broadened components of the water vapor continuum. The MT_CKD model has been updated in the microwave region to provide improved agreement with the measurements. MonoRTM has been updated accordingly. The results for the different instruments and frequencies were consistent, providing high confidence in the continuum updates. The estimated uncertainties on the updated continuum coefficients in MT_CKD are 4% on the foreign-broadened water vapor continuum and 4% on the self-broadened water vapor continuum.**

***Index Terms*—Microwave propagation, microwave radiometry, passive microwave remote sensing.**

I. Introduction

WELL-CALIBRATED microwave radiometers (MWRs) (satellite and ground based) have enabled measurements of long time series of geophysical parameters that are important for short-term weather forecasting and for studying the global hydrologic cycle, the Earth's radiation budget and climate. In order to correctly interpret the radiometer measurements in terms of geophysical parameters (atmospheric temperature and water vapor as well as surface and cloud parameters), the accurate modeling of atmospheric gaseous absorption is the key. Currently, the limiting factor on the accuracy of the modeling of microwave gaseous absorption using radiative transfer models is our knowledge of the associated spectroscopy (line parameters, line shape, and continuum).

The accurate modeling of continuum absorption is crucial for the so-called window regions of the spectrum, the relatively transparent regions between lines. The window regions in the microwave, particularly above 19 GHz, are of critical importance for Earth remote sensing and data assimilation, providing measurements for the determination of the liquid water path (LWP) [42] and near-surface wind speed over oceans as well as the characterization of sea ice and land surfaces (e.g., snow) from satellites. The window regions are also important for the measurement of the LWP from the ground [20]. The accurate modeling of the continuum absorption is particularly important in the measurement of the LWP for clouds with low water optical depths, due to the relatively large contribution of the continuum to the total optical depth. These "thin" liquid water clouds play an important role in the determination of the radiative energy balance of the Earth (see, e.g., [36], [37], and references therein) and exhibit extensive coverage of the globe. For example, a study of the distribution of the LWP at a continental midlatitude site showed that 50% of the liquid water clouds over that site have a LWP less than $100\ \mathrm{g \cdot m^{-2}}$ [22].

Molecules with a significant continuum in the microwave region include water vapor, nitrogen, and oxygen. Of these, the water vapor continuum is subject to the largest uncertainty. Laboratory measurements of the water vapor continuum are made difficult by the long path lengths required with conventional spectroscopic techniques or by the complexities encountered with methods of high sensitivity. From a theoretical point of view, the continuum has posed a relatively complex problem [3]. The Mlawer, Tobin, Clough, Kneizys, and Davis (MT_CKD) continuum model (see Section II-B) was developed to exploit the available theoretical and experimental information. It is a semiempirical model, constrained by the known physics, with the same line shape used for all spectral regions from the microwave to the ultraviolet while also constrained by laboratory and field measurements.

Given an underlying model of the continuum (such as that provided by the MT_CKD formulation) and reasonable estimates from laboratory measurements, ground-based radiometer measurements provide a critical means for validating and refining values of the continuum coefficients. Although there may be difficulties associated with adequately characterizing the atmospheric path and with accurate stable instrument calibration,

Manuscript received December 7, 2009; revised May 21, 2010 and July 2, 2010; accepted September 22, 2010. Date of publication January 5, 2011; date of current version May 20, 2011. This work was supported in part by the Office of Biological and Environmental Research of the U.S. Department of Energy as part of the Atmospheric Radiation Measurement Program and in part by the Joint Center for Satellite Data Assimilation.

The authors are with Atmospheric and Environmental Research, Inc., Lexington, MA 02421 USA.

Color versions of one or more of the figures in this paper are available online at http://ieeexplore.ieee.org.

Digital Object Identifier 10.1109/TGRS.2010.2091416

atmospheric measurements can provide the long path lengths necessary for the assessment of water vapor continuum absorption. Ground-based measurements, viewing the atmosphere against a background of cold space, are not subject to the difficulties in the characterization of surface emissivity associated with space-based measurements. In addition, ground-based measurements offer the opportunities for a range of coincident measurements for the characterization of the atmospheric state, provide the advantage of better temporal and spatial colocation with *in situ* profile measurements (from radiosondes), and minimize the issues of representativeness, since the field of view of the ground-based instruments covers a relatively small area over the altitude range over which most of the water vapor is concentrated.

In this paper, measurements from ground-based radiometers situated at two Atmospheric Radiation Measurement (ARM) Program sites are used in conjunction with radiosonde profiles and a radiative transfer model to assess the current capability in modeling the water vapor continuum absorption, to determine values for the self- and foreign-broadened water vapor continua that are most consistent with the radiometric measurements, and to provide a realistic estimate of the uncertainty associated with these values.

Section II provides a background on the "monochromatic radiative transfer model" (MonoRTM) and the MT_CKD continuum model used in this paper. Section III describes the data sets, the approach used, and the results obtained in determining the continuum coefficients that best fit the available data. Section IV provides some discussion of the implications of the results, while Section V provides a summary of this paper and some concluding remarks.

II. Model Description and Background

A. MonoRTM

The radiative transfer model used in this paper is MonoRTM, developed and distributed by Atmospheric and Environmental Research, Inc. The model is publicly available and may be downloaded from http://rtweb.aer.com. MonoRTM was designed to process one or a number of monochromatic frequencies. Although the model was initially developed for use in the microwave region, MonoRTM versions numbered v4.0 onward may be used at any frequency from the microwave to the ultraviolet. MonoRTM is based on the same physics as that of the well-known Line-By-Line Radiative Transfer Model (LBLRTM) [6], [32]. MonoRTM may be used to calculate the radiances associated with the atmospheric absorption by molecules in all spectral regions and with the cloud liquid water in the microwave.

Spectral line parameters are based on HITRAN 2004 with a few selected exceptions, namely, the parameters for the oxygen lines and for the four strong water vapor lines at 22, 183, 325, and 380 GHz. The oxygen line widths and line coupling coefficients are from [33] and have been validated using ground-based radiometers [8], [9]. The line strengths for the 22- and 183-GHz water vapor lines are based on an analysis of the Stark-effect measurements described in [7]. The air-broadened half width for the 22-GHz water vapor line is from [26], while the half widths of the 183- and 325-GHz lines are from a calculation by R. R. Gamache (described in [26]). The self-broadened half width of the 325-GHz line is from [15]. Both the air- and self-broadened half widths of the 380-GHz line are from [15]. The temperature dependences of the half widths and the pressure shifts for these four water lines are from Gamache's calculations (described in [26]). MonoRTM has been extensively validated using ground-based measurements from the Department of Energy's ARM Program [6], [8], [9], [11], [26].

For each monochromatic calculation in MonoRTM, the local line contribution is calculated for each line within $+/-25$ cm^{-1} from the chosen frequency. Contributions outside $+/-25$ cm^{-1} are accounted for by the MT_CKD continuum (see Section II-B); thus, the continuum and the details of the line-by-line calculation are inextricably related.

Fig. 1 shows the contributions of different atmospheric constituents in the microwave region, calculated using MonoRTM, for a U.S. Standard Atmosphere (where the precipitable water vapor (PWV) is 1.4 cm). The main features in the spectrum are the water vapor lines at 22, 183, 325, and 380 GHz, the 60-GHz oxygen band, and the 118-GHz oxygen line. (There are also a number of strong oxygen lines around 0 GHz that do not contribute strongly to the optical depth due to the small magnitude of the radiation field there.) Contributions from the lines of other molecules, such as ozone and nitrous oxide, are very small in comparison but can be nonnegligible for extremely dry atmospheres.

B. MT_CKD Continuum

MonoRTM uses the MT_CKD continuum model. The MT_CKD continuum [6], a successor to the Clough, Kneizys, and Davis continuum model [2], [3], is widely used within the radiative transfer modeling community. The original CKD model, CKD 0 [2], [3], was developed on the premise of a single line shape associated with each water vapor monomer absorption line for foreign broadening and a second line shape for the self-broadening. Each of these line shapes required absorption in excess of that provided by the Lorentz line shape in the intermediate wing region, within $\sim$100 cm^{-1} of the line center, in order to provide agreement with the measurements within various water vapor bands. The details of the line shape formulation for the allowed line contribution and the rationale for the choice of this formulation can be found in [3]. A key feature of this formulation is the clear separation of the radiation field term from the symmetrized power spectral density function [39]. The spectral density function has the same form across all spectral regions, and the main differences between regions arise from the form of the radiation field. The continuum absorption is then defined by excluding from the power spectral density function the spectral components associated with the local line contribution (defined for each line within $+/-25$ cm^{-1} from the central frequency.)

Over time, a significant modification to this approach was implemented for two important reasons: 1) More degrees of freedom were required to fit the data than were available in the original line shape, and 2) the super-Lorentzian line shape in

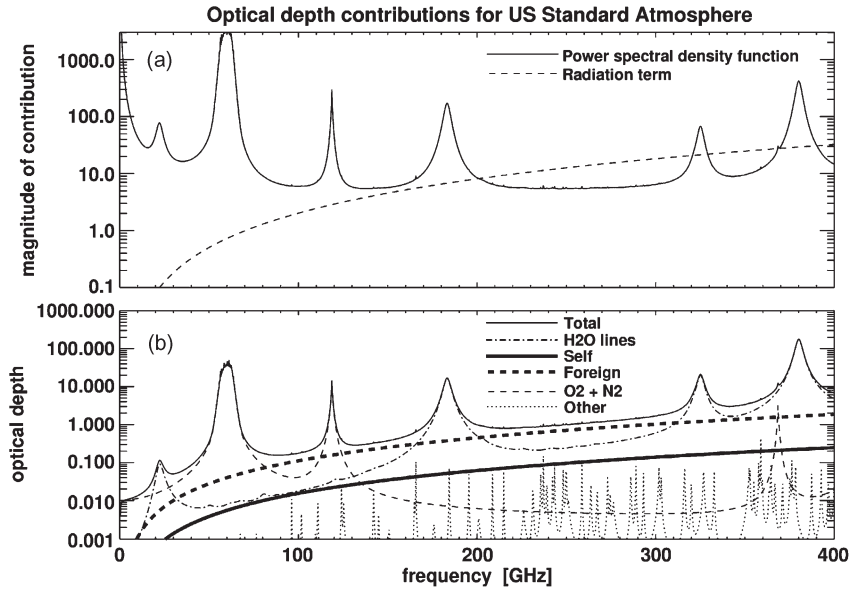

Fig. 1. Optical depth contributions from a MonoRTM calculation using the U.S. Standard Atmosphere. (a) Contributions from the power spectral density function and the radiation term. (b) Optical depth contributions from different absorbers.

TABLE I
VERSION NUMBERS AND RELEASE DATES OF THE MONORTM VERSIONS DISCUSSED IN THIS PAPER, WITH ASSOCIATED CONTINUUM VERSION NUMBERS

MonoRTM version	Release date	Associated continuum version
MonoRTM v4.0	September 2008	MT_CKD v2.1
MonoRTM v4.2	July 2009	MT_CKD v2.4

the intermediate wing region was not supported by any known physics. To address these two issues, a collision-induced component to the continuum was developed to provide the excess absorption observed in the central region of the vibrational bands. The continuum behavior in between water vapor bands, known from measurements to be less than that associated with the far wing behavior of the Lorentz line shape, is provided by a second line shape applied to each allowed water vapor line. These two components, from collision-induced and allowed transitions, are both present in the MT_CKD formulation of the foreign as well as the self-broadened continuum and provide the additional degrees of freedom necessary to fit the observations. The primary impetus for this revision was to restore the consistency between the formulation and the improved measured continuum values. The resulting updated model has now been publicly available for a number of years [6]. Table I shows the continuum versions associated with the MonoRTM versions discussed in this paper.

The MT_CKD continuum model is semiempirical, fitted using a range of laboratory and atmospheric measurements while constrained by the known physics. Consistent line shapes are used for all lines from the microwave to the ultraviolet, ensuring that the underlying physics is consistent across the spectral regions. Consistency between the spectral regions is a key consideration for a number of fields, for example, in the assimilation of a range of satellite radiances in the context of numerical weather prediction.

Fig. 2 shows the continuum coefficients at 296 K as a function of frequency. As stated earlier, the radiation term (with its temperature dependence) is removed for the definition of the continuum used here. Once the continuum coefficient has been defined in this way, empirical evidence indicates that the temperature dependence of the foreign continuum is small but that there is a need to account for the temperature dependence of the self-broadened continuum. The ratio of the self-coefficient at 296 K to that at 260 K at zero frequency is around 0.62. The variation of the temperature dependence with frequency is negligible over the spectral range shown in Fig. 2. The continuum coefficients are stored every 10 cm^{-1} (approximately every 300 GHz). It is clear from Fig. 2 that, in this formulation, the continuum does not show strong spectral variation. The original CKD continuum was constrained to fit the experimental data of Burch [1], and the values of the power spectral density function at zero frequency were originally based on the available laboratory measurements. However, over the years, the values of the spectral density function for the self-broadened continuum in the microwave region, including at zero frequency, have been subject to adjustments (see Fig. 2) as new measurements became available both in the microwave and in other spectral regions. While the value of the power spectral density function for the foreign-broadened continuum at zero frequency had remained unchanged from CKD 0 until this work, small adjustments to the foreign continuum in the microwave region have occurred over time.

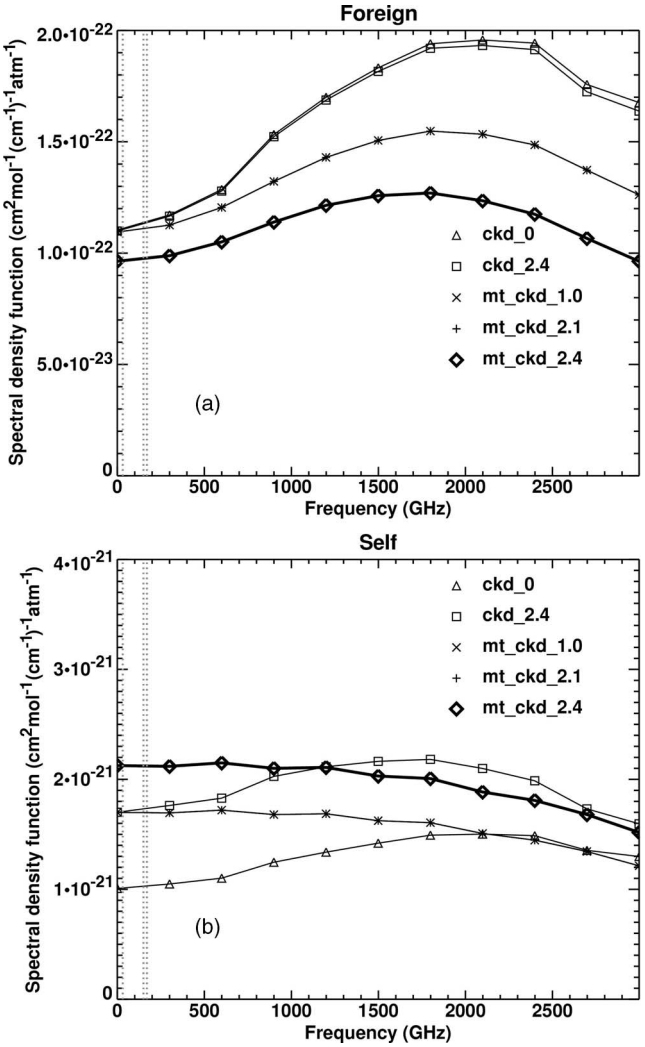

Fig. 2. Continuum coefficients at 296 K as a function of frequency for the foreign- and self-broadened water vapor continua, showing past and current versions of the continuum in the microwave region and beyond. (Note that there were no changes between MT_CKD v1.0 and MT_CKD v2.1 in this frequency range.) Moreover, marked with vertical dotted lines are the frequencies of the instrument channels used for continuum validation in this paper.

New constraints on the foreign- and self-broadened water vapor continua for this paper are provided by the ground-based microwave measurements of downwelling atmospheric radiation from 30 to 170 GHz (0 to 5.7 cm^{-1}). At higher frequencies, the next spectral region where such ground-based measurements in regions with sufficient transparency for continuum validation have been available is the far infrared (IR) [12], [31]. New results from the second phase of the Radiative Heating in Underexplored Bands Campaign (RHUBC) [34] are expected to extend such measurements down to $\sim$200 cm^{-1} in the far IR, as well as provide measurements in the terahertz and microwave regions, which will lead to valuable additional constraints on the MT_CKD continuum formulation in the future.

III. MonoRTM and the MT_CKD Continuum in the Context of Other Models

The goal of this paper was to assess and improve the knowledge of the water vapor continuum in the microwave region. Resulting updates have been implemented in the MT_CKD continuum model and, therefore, in MonoRTM. A range of different microwave radiative transfer models is in use within the community, and there are a large number of studies in the literature dealing with comparisons between different models as well as between models and data [14], [22], [24], [43]. This paper is not intended to be a model comparison paper. However, for reference, we present comparisons between MonoRTM and the widely used Rosenkranz microwave radiative transfer model [29], [30]. The Rosenkranz model has heritage in the Liebe microwave propagation model (MPM) [16], [17] but has been maintained and updated in recent years. The water vapor continuum in the Rosenkranz model is a combination of the components of the continua in the 1987 and 1993 versions of the Liebe MPM, although some other aspects of the model (such as the number of molecules and absorption lines) have been updated in recent years. The version of the Rosenkranz model shown in this paper is the one described in [29].

MonoRTM and the Rosenkranz model are formulated differently and use different spectroscopic line parameters as well as different continuum models. For the purposes of this paper, the most significant differences between them are the water vapor continuum and the value used for the 22-GHz line width. MonoRTM uses the value described in [26] for the 22-GHz line width, while the Rosenkranz model uses a higher value from [18]. A more detailed discussion of width values in the literature can be found in [26]. The focus of this paper is on the water vapor continuum. In the analysis that follows, the parts of the optical depth contribution labeled within the models as water vapor continuum absorption have been compared. It is very important to note that the continuum and the details of the line-by-line calculation in any model are inextricably related.

Fig. 3 shows the ratios of the optical depth due to different formulations of the foreign- and self-broadened water vapor continua relative to MT_CKD v2.1 (MonoRTM v4.0). The optical depth calculations were performed for a single layer at a uniform temperature. Note that the differences between continuum formulations may be dependent on both the frequency and temperature. For example, Fig. 3 demonstrates the difference in the temperature dependence for the self-broadened water vapor continuum between MT_CKD, the Rosenkranz model, and the model used by Remote Sensing Systems (RSS), an empirically adjusted version of the Rosenkranz model used in the Advanced Microwave Scanning Radiometer (AMSR) algorithm [23], [41]. The temperature dependence of the self-broadened continuum in the MT_CKD is empirically determined using laboratory measurements as constraints.

IV. Assessment of Continuum Uncertainty

In this paper, measurements from ground-based radiometers situated at two ARM Program sites are used in conjunction with radiosonde temperature and humidity profiles and a radiative transfer model to assess the current capability in modeling the water vapor continuum absorption, to determine values for the self- and foreign-broadened water vapor continua that are most consistent with the radiometric measurements, and to provide

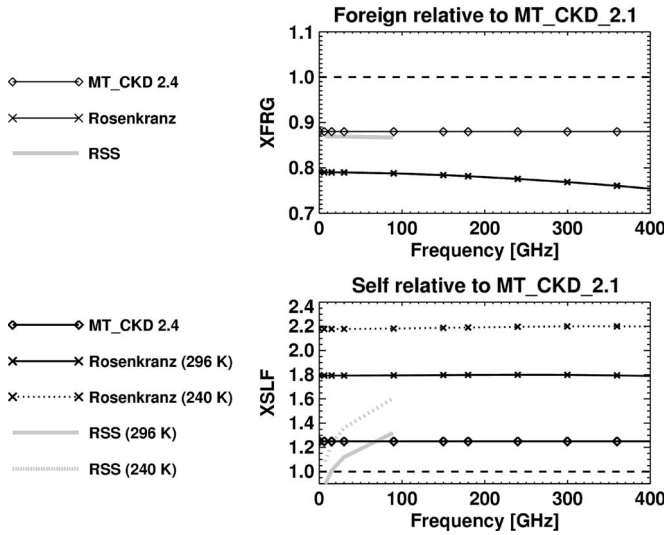

Fig. 3. Ratios (XFRG and XSLF) of optical depth due to different formulations of the (a) foreign- and (b) self-broadened water vapor continua, relative to the MT_CKD v2.1 continuum (MonoRTM v4.0). Optical depth calculations were performed for a single layer at a uniform temperature. (The RSS model is an empirical adjustment to the Rosenkranz model, derived from satellite channels in the frequency interval of 7–90 GHz.) The solid lines show the ratios of the continuum optical depths at 296 K. The dotted lines in (b) show the ratio at 240 K in order to demonstrate the effect of the different temperature dependence of the self-broadened continuum in the Rosenkranz model compared to that in the MT_CKD formulation.

a realistic estimate of the uncertainty associated with these values.

Since, in many cases, radiosonde humidity profiles offer the best available estimate of the vertical profile, radiosonde profiles are often considered as the "truth." However, inconsistencies between measurements by different types of profilers, or even in profiles recorded by the same type of instrument, have been repeatedly noted (see [35] and references therein). Examples include significant site-specific biases in humidity profiles noted during the Tropical Ocean Global Atmosphere Coupled Ocean–Atmosphere Response Experiment observations [21] as well as the dry bias in Vaisala RS80 humidity profiles revealed during a long-term study at the ARM Southern Great Plains (SGP) site [35]. Determining the source of such inconsistencies and developing methods to remove them have been the focus of much research in recent years [10], [25], [40]. In addition to any general systematic biases, comparisons between the measurements from the ground-based MWRs and the radiative transfer models using radiosonde profiles as input show considerable scatter. Scaling the radiosonde profiles according to the total PWV retrieved from MWRs in the 22-GHz region has been shown to be an effective approach in addressing both the bias and the scatter [6], [36], [37]. In this paper, this scaling approach has been used to reduce the scatter in model/measurement comparisons in order to derive information on the self- and foreign-broadened water vapor continua.

A range of ground-based radiometer measurements was used to assess the water vapor continuum in the microwave region and to determine continuum values that provide the best fit across different frequencies and atmospheric conditions. The key instruments used were the two-channel MWR, an instrument built by Radiometrics (http://www.radiometrics.com) with double sideband channels at 23.8 and 31.4 GHz, the two-channel "MWR at high frequencies" (MWRHF) built by Radiometer Physics GmbH (RPG) with channels at 90 and 150 GHz, and the Radiometrics "microwave profiler at 183 GHz" (MP183), i.e., a G-band vapor radiometer profiler (GVRP) with fifteen single sideband channels between 170 and 183.31 GHz. The data sets are summarized in Table II and are described in greater detail hereinafter.

For each data set, available clear-sky radiosonde profiles were scaled to provide agreement with the 23.8-GHz MWR channel. The scaled radiosondes were then used as input to MonoRTM, and the residuals (measured minus the modeled brightness temperature) in the relevant window channels were plotted as a function of PWV. The resulting shape of the residuals as a function of PWV for channels where the absorption is dominated by continuum absorption can provide some insight into the continuum. The foreign-broadened continuum absorption scales linearly with water vapor, while the self-broadened continuum absorption increases with the square of the water vapor. At lower water vapor amounts, the foreign continuum absorption dominates over the self-broadened continuum absorption. The contribution from the self-broadened continuum becomes increasingly important as the water vapor amount increases. This concept is demonstrated in Fig. 4. Measurements over a broad range of water vapor values are needed in order to distinguish between any possible errors in the foreign- and self-broadened continua [5].

The MWR data set at the SGP has by far the widest range of water vapor conditions available (see Table I). The MWR is also the longest running instrument of the three and therefore provides not only the largest number of clear-sky cases but also a long history and a high degree of confidence in the instrument calibration. It can be seen from Fig. 2 that the continuum is not expected to show a great deal of spectral variation in the region spanned by the data sets used here. Therefore, we regard the 31.4-GHz data set from the MWR at the SGP to be the one that should provide the most accurate continuum information, with the smallest uncertainty. The other data sets provide checks on consistency.

Previous work [5], using scaled RS80 radiosondes, has demonstrated that the self- and foreign-broadened water vapor continua in the Rosenkranz model could not be consistent with the ground-based radiometer measurements from the ARM SGP site between 1998 and 2000, while the CKD_2.4 continuum within MonoRTM v2.2 offered consistency with measurements within the estimated measurement uncertainty. In this paper, new radiometer measurements have been used with scaled RS92 radiosondes (known to be an improvement over the RS-80s) to update the MT_CKD continuum as used in a more recent version of MonoRTM.

A. MWR Instrument and Continuum Validation at 31.4 GHz

The two-channel (23.8- and 31.4-GHz) MWR system has a long and successful history within the ARM Program and has been providing PWV and LWP retrievals at ARM sites for over 15 years. There is currently an MWR present at all of the ARM sites. These instruments are automatically calibrated

TABLE II
SUMMARY OF DATA SETS USED FOR CONTINUUM VALIDATION

Instrument	Channel frequency (GHz)	Location	Dates	Sonde PWV range (cm)	Range of mean atmospheric temperatures	Range of water vapor weighted temperatures	Number of clear sky cases
MWR	31.4	SGP	01/05-12/07	0.15-5.0	240-285 K	257-297 K	1218
MWRHF	150	FKB	06/07-12/07	0.37-2.8	240-262 K	262-286 K	35
GVRP	170	SGP	01/08-03/08	0.27-2.1	243-267 K	258-285 K	77

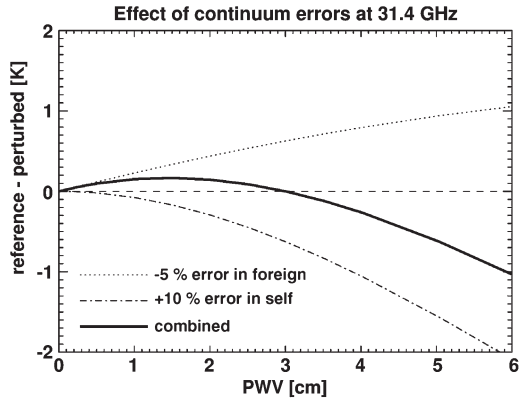

Fig. 4. Potential cancellation of errors between the self- and foreign-broadened water vapor continua.

using the "tipping curve" or "tip cal" method [13]. Robust data quality checks and thousands of "successful" tip calibrations help to ensure the good stable calibration of the radiometer [19]. The quoted measurement accuracy is 0.3 K. The MWRs are equipped with a heater/blower mechanism that directs warm air over the radome to prevent the formation of dew on the radiometer.

The MWR data set used here is from the ARM SGP site in Oklahoma. The time period used in this paper for the 31.4-GHz continuum validation was January 1, 2005 to December 31, 2007. During this period, Vaisala RS92 radiosondes were launched four times per day from the SGP site. For the comparisons with MonoRTM, the MWR-measured brightness temperatures were averaged from 5 min before to 30 min after the radiosonde launch, in order to account for varying atmospheric conditions in the time that it took for the radiosonde to reach its upper altitudes. The profiles were screened for liquid cloud by examining the standard deviation of the 31.4-GHz channel brightness temperatures over the time window around the sonde launch used for averaging. The test for the standard deviation follows that described in [36] and [37]; if the standard deviation is less than $a + b * \text{PWV}$, where $a = 0.15$ K, $b = 0.06$ K/cm, and the PWV is calculated from the sonde, then the sample is assumed to be clear. Additional screening for cloud was performed using colocated ceilometer data.

Fig. 5(a) and (b) shows the MWR residuals (measured minus the modeled brightness temperatures) using MonoRTM v4.0 for this SGP data set using "raw" clear-sky radiosonde profiles as input. Both channels show an overall negative bias in the residuals as well as significant scatter. The negative bias in the 23.8-GHz channel, where the absorption is dominated by the line contribution rather than the continuum, is due to an overall dry bias in the radiosondes, while the scatter is due to the uncertainty that varies from sonde to sonde. The 31.4-GHz window channel, where the absorption is dominated by the continuum contribution, could be affected both by the dry bias in the radiosondes and by the errors in the continuum. In order to determine values for the self- and foreign-broadened water vapor continua that would provide the best fit to the data, model/measurement comparisons were performed with combinations of different scaling factors applied to the self- and foreign-broadened water vapor continua in MT_CKD 2.1. For each set of continuum scaling factors, an initial "raw" run was performed. In order to separate the radiosonde uncertainties from the continuum uncertainties in the 31.4-GHz channel, PWV scaling factors were retrieved from the 23.8-GHz channel measurements. The model was run with the scaled radiosonde water profiles as input, and the 31.4-GHz channel brightness temperature residuals were examined in order to assess the quality of the continuum fit. The quality of the fit to the 31.4-GHz data was defined using a cost function J_1 consisting of three terms. The first term is a "sum of squares" that takes account of the distance of each individual residual point from zero. In some cases, it is visually obvious that the residuals for one set of scaling factors are worse than those for another set due to an obvious systematic shape in the envelope of the residual points, but a simple sum-of-squares term may not distinguish well which one is better. The cost function therefore also includes terms to weight against the slope and curvature in the fit to the entire data set

$$J_1 = (\mathbf{y} - \mathbf{F})^T \mathbf{S}_m^{-1} (\mathbf{y} - \mathbf{F}) + 100 \times s^2 + 1000 \times c^2$$

where $\mathbf{y}$ is the vector consisting of all 31.4-GHz measurements and $\mathbf{F}$ is the corresponding forward model vector from the MonoRTM calculations. $\mathbf{S}_m$ is the measurement noise covariance matrix, which, in this case, is a diagonal matrix with values of $(0.3\ \text{K})^2$ along the diagonal. The values s and c are the linear ("slope") and quadratic ("curvature") coefficients of a second-order polynomial calculated from a singular value decomposition fit [28] to the entire set of 31.4-GHz residuals. These s and c terms help to compensate for the fact that the distribution of PWV values for this data set is heavily weighted

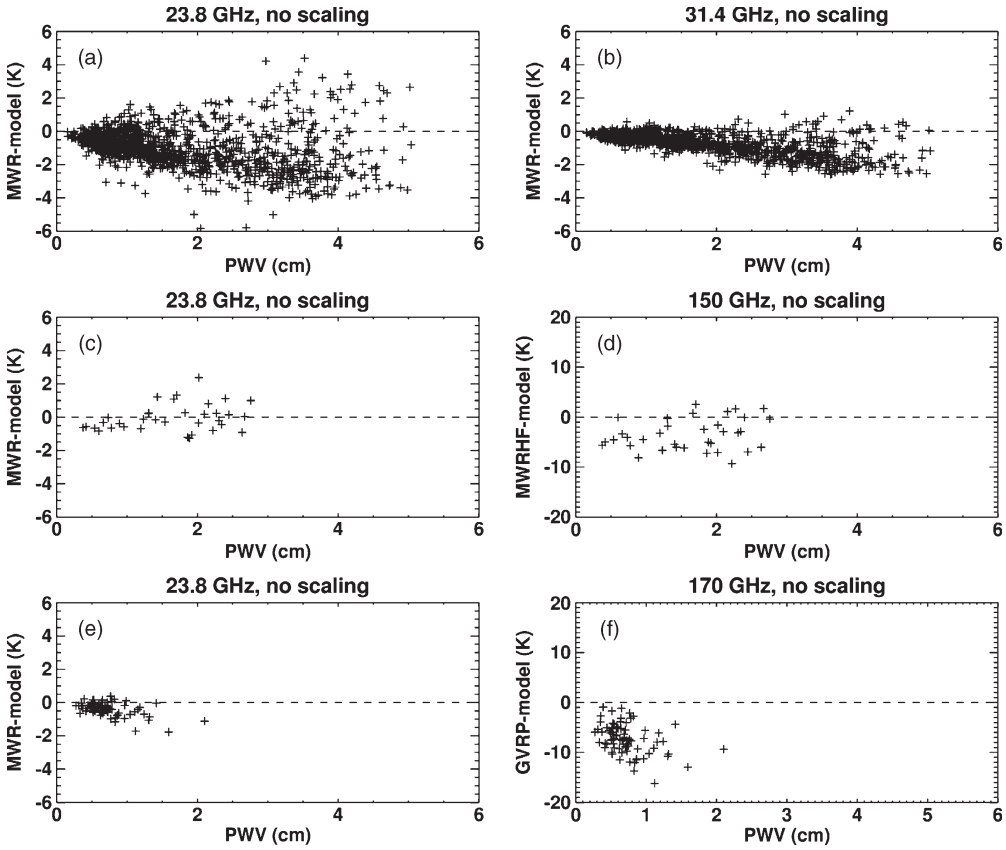

Fig. 5. Plots showing "raw" (unscaled radiosonde) comparisons for the 23.8-GHz MWR channel used for PWV scaling and for the continuum-dominated channel. (a) and (b) SGP data set from 2005 to 2007 using the MWR 31.4-GHz channel. (c) and (d) COPS data set using the MWRHF 150-GHz channel. (e) and (f) SGP data set from January to March 2008 using the GVRP 170-GHz channel. Note the larger y-axis scales for the 150- and 170-GHz comparisons. The residuals shown here are for MonoRTM v4.0.

toward drier values. The weighting factors for the s and c terms were chosen in order to make these terms comparable in magnitude to the sum-of-squares term for continuum scaling combinations where the slope and/or curvature in the residuals was readily apparent from visual inspection.

Note that the PWV retrievals performed for this paper are not quite the same as the ARM operational PWV retrievals at the SGP site. In the ARM operational retrievals of the PWV and LWP from the MWR (which use MonoRTM as the forward model), a time-dependent bias offset is applied to the 23.8-GHz observations before any retrievals are performed. The purpose of this bias offset is to attempt to reduce any bias in the retrieved PWV that might result from a systematic bias in either the model or in the observations. The method requires a large number of clear-sky radiosonde observations and is described in detail in [36] and [37]. The radiosondes, the MWR calibration, and MonoRTM (notably the oxygen spectroscopy used in the model) have all been subject to improvements over the years since the operational ARM PWV retrievals began, and the bias offsets calculated have been small (less than 0.5 K) in recent years. Based on the results in Fig. 5(a), we have decided to assume that the instrument and the model are in agreement at zero PWV and have not applied a bias offset to the 23.8-GHz channel before our PWV retrievals.

Fig. 6 shows the offsets for each scaling combination calculated for the whole three-year data set using a second-order polynomial fit to the 23.8-GHz residuals. A polynomial fit is

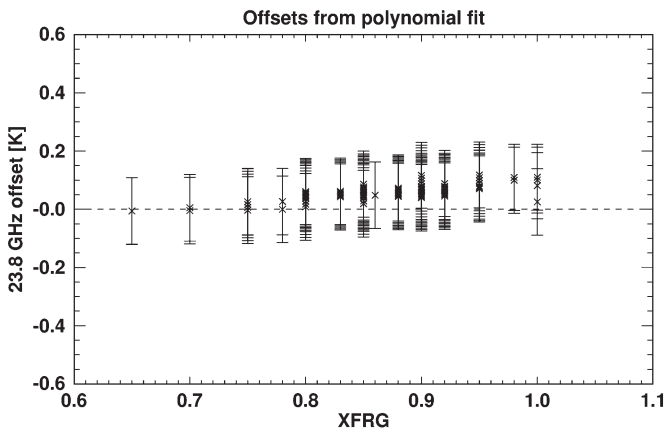

Fig. 6. Bias offset values for the 23.8-GHz channel, calculated using a second-order polynomial fit to all three years worth of data. Error bars show the one sigma uncertainty on the fitted offset for each self/foreign scaling combination. XFRG denotes the scaling factor applied to the foreign continuum. The multiple points plotted for each abscissa value show different values of the self-scaling (XSLF) applied for each value of XFRG.

our preferred method for the assessment of offsets in this large data set since this method fits the residuals at zero PWV and should therefore be the least sensitive to the uncertainties in the raw sonde values and to the water vapor continuum values used. Alternative methods involving the average of points with PWV below some threshold were rejected due to the inherent sensitivity of nonzero PWV residuals on the continuum used.

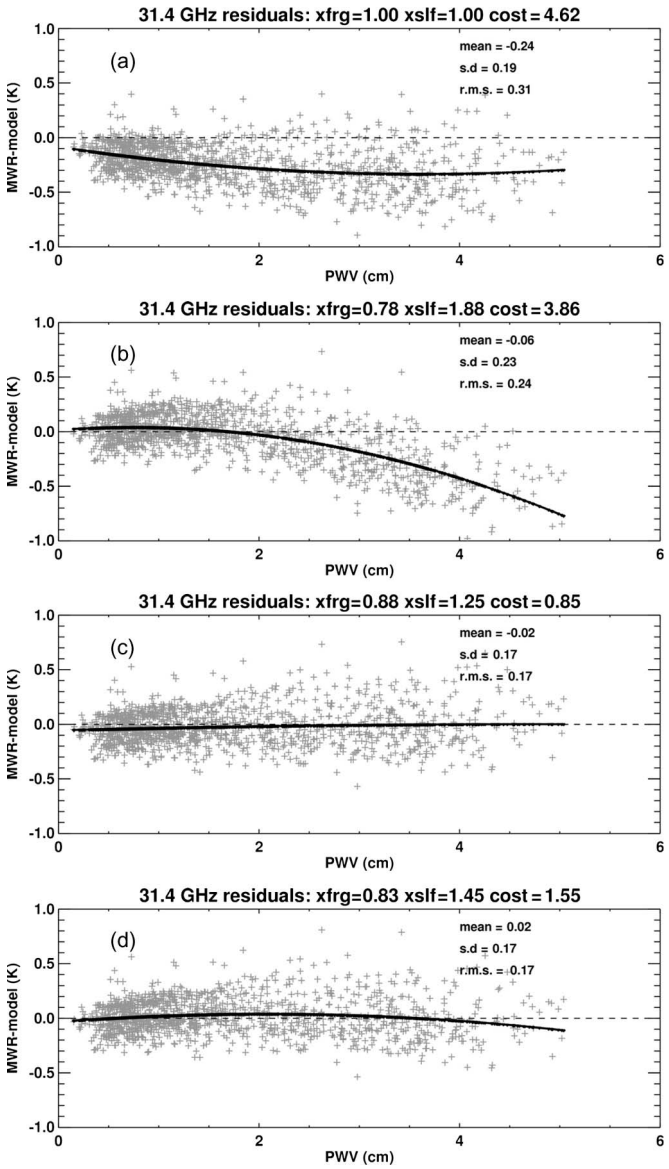

Fig. 7. Sample MWR residuals for different continuum scaling factors. (a) MT_CKD v2.1 continuum. (b) Scaling factors equivalent to Rosenkranz-like continuum at a representative temperature for this data set. (c) "Best fit" continuum scaling factors adopted for MT_CKD v2.4. (d) Continuum scaling factors that result in the lowest absolute rms value. The visible curvature in the residuals in (d) demonstrates the need for a cost function that weights against the curvature.

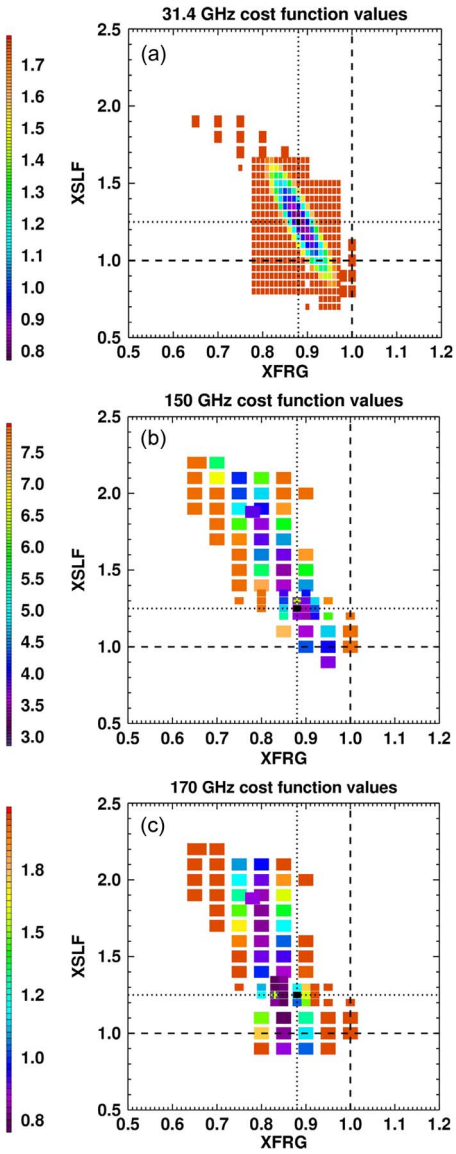

Fig. 8. Cost-function surfaces for different scaling factors applied to the MT_CKD 2.1 self (XSLF)- and foreign (XFRG)-broadened water vapor continua at (a) 31.4 GHz, (b) 150 GHz, and (c) 170 GHz. Crosshairs with dashed lines show positions of the MT_CKD_2.1 values, while crosshairs with dotted lines show positions of the MT_CKD_2.4 values.

Based on Fig. 6, we conclude that any bias offset in the instrument is small and that 0.5 K is a pessimistic uncertainty estimate for the bias offset.

Fig. 7 shows sample 31.4-GHz residuals from using scaled sondes for different combinations of continuum scaling. The four example cases shown are MT_CKD 2.1 (a), some "Rosenkranz-like" continuum scaling values (b), the values deemed to provide the best fit to the data (c), and the values that provide the smallest rms residual error (d). Note that the residuals shown in (b) are not from the Rosenkranz model—they are from the MonoRTM with the MT_CKD 2.1 self- and foreign-broadened water vapor continua scaled to approximate the water vapor continuum in the Rosenkranz model. The curvature evident from the visual inspection of the residuals in Fig. 7(d) illustrates the need for additional "slope" and "curvature" terms in the cost function. With a data set more strongly weighted toward higher PWV values, these extra terms would likely not be necessary.

Fig. 8(a) shows a 2-D representation of the surface of the cost function J_1. (Values with $J_1 > 1.7$ are all shown in red.) The surface has a clear and well-defined minimum for scaling factors (applied to MT_CKD 2.1) of 0.88 for the foreign-broadened continuum and 1.25 for the self-broadened continuum. A parabolic cost function surface was fitted to the points shown in Fig. 8, and a second-order polynomial ($y = a + bx' + cx'^2$) was fitted to the major and minor axes of the equal-cost ellipses, where x' is the coordinate along an ellipse axis. The position of the minimum along the ellipse axis is therefore given by $x' = -b/(2c)$. The 1-sigma errors in the fitted parameters (b, c) were added in quadrature to calculate

an estimate of the error in the position of the minimum. This gives uncertainties of σ_{a} and σ_{b} along the major and minor axes of the ellipse, respectively. The variances of the projection of these uncertainties onto the x (foreign)- and y (self)-axes are then given by

$$\sigma_x^2 = (\sigma_a \cos\alpha)^2 + (\sigma_b \sin\alpha)^2$$
$$\sigma_y^2 = (\sigma_a \sin\alpha)^2 + (\sigma_b \cos\alpha)^2$$

where α is the angle between the major axis of the ellipse and the x-axis (in this case, 78°). This yields estimated errors of 1% in the foreign-broadened continuum and 4% in the self-broadened continuum. These numbers are underestimates of the total error. They do not account for possible biases in the continuum estimates that could arise from systematic errors inherent in the assumptions used in this method. The two largest sources of systematic uncertainty to consider in this spectral region are the bias offset (discussed earlier—which could include both instrument effects and errors in the modeling of oxygen and nitrogen absorption) and the width of the 22-GHz line. The uncertainty on the bias offset has been estimated at 0.5 K, while the uncertainty on the 22-GHz line width is estimated as 1.6% [26].

An analysis was performed to quantify the impact of these two systematic errors on the implied best fit continuum scaling. The effect of the addition of a 0.5-K bias offset to the MWR 23.8-GHz channel is to reduce the best fit scaling value for the foreign-broadened continuum by 3% (from 0.88 to 0.85). The impact of the offset on the best fit to the self-broadened continuum is negligible. This is because the fit to the self-broadened continuum is largely governed by the curvature in the residuals as a function of PWV, and the offset has minimal impact on this curvature. It is interesting to note that the values of the cost function (not shown) are somewhat higher when the bias offset is applied to the data, which provides some support to the decision not to apply a bias offset. The effect of a 1.6% increase in the width is also the reduction of the best fit scaling value for the foreign-broadened continuum by 3%. Again, the impact on the fit to the self-broadened continuum scaling is negligible. However, an increase in the width value does not impact the magnitude of the minimum value of the cost function attained.

Adding these errors in quadrature, the combination of the 1% from the fitting of the cost minimum, the 3% from the bias offset uncertainty, and the 3% from the width uncertainty results in a total uncertainty estimate of around 4% for the foreign-broadened continuum. Neither of the systematic error sources considered has an appreciable impact on the fit to the self-broadened continuum. Therefore, we quote total error estimates of 4% on the foreign-broadened continuum and 4% on the self-broadened continuum.

B. Continuum Validation at 150 GHz

The MWRHF instrument has channels at 90 and 150 GHz. This ARM-owned instrument was deployed during the Convectively and Orographically-induced Precipitation Study (COPS) from the ARM mobile facility in the Black Forest, Germany (FKB) from July to December 2007. The bandwidth of the MWRHF channels is 2000 MHz, and the quoted measurement uncertainty is 0.5 K.

The MWRHF was occasionally calibrated during this time period by viewing a liquid nitrogen target. Observations from the target and from the internal blackbody (at ambient temperature) were used to determine both the system noise and the gain. The instrument was also performing regularly scheduled TIP scans [13]. The calibration of the MWRHF 150-GHz data was determined solely from the liquid nitrogen calibration events. The calibration of the 90-GHz observations included a mixture of liquid nitrogen and TIP scan calibrations. A postanalysis of the 90-GHz TIP calibration periods determined that many of these periods were actually not valid due to fog and dew accumulation on the radomes of the radiometers [34]. The calibration of the 90-GHz data was therefore neither constant nor accurate over time, so the 90-GHz MWRHF data were not used in this analysis.

Another 90/150-GHz RPG radiometer, fielded by the University of Cologne, was also operating at the FKB site during this time period. This second radiometer was calibrated in the same way as the MWRHF, but since the instruments were owned and operated by different organizations, the liquid nitrogen calibrations were performed by different instrument teams and at different times. The liquid nitrogen calibrations may therefore be considered to be independent. Turner *et al.* [34] performed a comparison between the 150-GHz data from the two radiometers and found good agreement between them, with a slope of 1.005 and a mean bias of 0.53 K. The measurements from the second radiometer were not used in the analysis presented here, but the comparison performed by Turner *et al.* [34] provides additional confidence in the MWRHF data set.

A large number of other measurements were also being made at the FKB site during the COPS, including those from a two-channel MWR, a ceilometer, surface meteorology, backscatter observations from a micropulse lidar, and radiance observations from an IR interferometer. (IR interferometer measurements have excellent sensitivity to small amounts of liquid water.) The same subset of MWRHF 150-GHz observations used by Turner *et al.* [34], carefully screened for dew and cloud, has been used in this paper.

The screening for cloud left 35 clear-sky radiosonde matches with the MWRHF data. PWV scaling factors were retrieved for each of these radiosonde humidity profiles using the 23.8-GHz channel of the colocated MWR. As with the 31.4-GHz SGP analysis presented earlier, the decision was made not to apply a bias offset to the 23.8-GHz data before retrieving the PWV scaling factors. The "raw" comparisons at the MWR 23.8-GHz and MWRHF 150-GHz channels from the COPS data set are shown in Fig. 5(c) and (d). Viewed in isolation, Fig. 5(c) could be considered to suggest that a bias offset of around 1 K would be appropriate for the 23.8-GHz channel. However, when viewed alongside the MWR SGP 23.8-GHz residuals shown in Fig. 5(a), it is clear that this small set of 35 points could easily lie within the larger distribution of points in Fig. 5(a), and the data set shown in Fig. 5(a) does not support a bias offset as large as 1 K. The comparison of

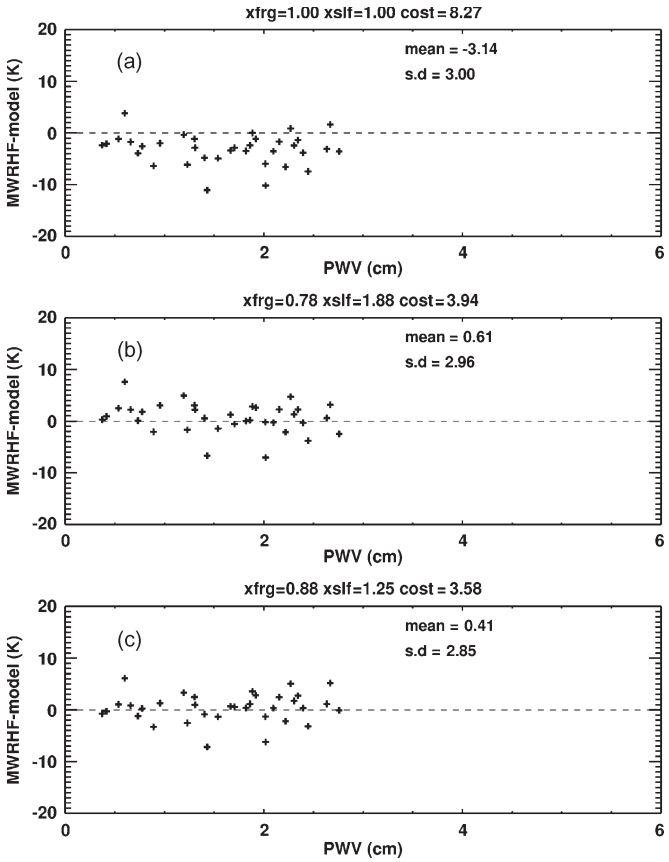

Fig. 9. Residuals at 150 GHz for different continuum scaling factor combinations. (a) MT_CKD v2.1. (b) Scaling factors equivalent to Rosenkranz-like continuum at a representative temperature for this data set. (c) "Best fit" continuum scaling factors adopted for MT_CKD v2.4.

Fig. 5(a) and (c) demonstrates issues associated with trying to draw conclusions from a small data set. The negative bias in the 150-GHz residuals in Fig. 5(d) is partly due to the radiosonde bias as discussed in Section IV-A and partly due to the continuum errors in MT_CKD v2.1, which result in larger brightness temperature residuals at this higher frequency than at 31.4 GHz.

The same procedure was followed for the 150-GHz continuum validation as for the 31.4-GHz validation. PWV scaling factors were retrieved using the 23.8-GHz MWR channel, these factors were applied to the sonde profiles, and the model/measurement results were compared at 150 GHz. Fig. 9 shows the MWRHF 150-GHz residuals (after the scaling of the sonde profile using the 23.8-GHz MWR channel) for different continuum scaling factors. The scatter in these residuals is higher than the expected instrument noise of 0.5 K. While the 23.8-GHz measurements depend mainly on the column water vapor, at 150 GHz, there is greater sensitivity to the atmospheric profile. The observed scatter is likely due to atmospheric representation errors (errors in the temperature/water vapor profile).

As with the MWR 31.4-GHz SGP data set, a cost function was used to determine the quality of the fit to each combination of continuum scaling factors. Unlike the MWR SGP data set, the MWRHF COPS data set does not contain a sufficient number of points or a sufficient range of PWV to reliably fit a curve to the residuals. Therefore, the cost function J_2 used here did not include terms associated with a fitted curve

$$J_2 = (\mathbf{y} - \mathbf{F})^T \mathbf{S}_m^{-1} (\mathbf{y} - \mathbf{F}).$$

In this case, the measurement covariance matrix S_{m} is a diagonal matrix with values of $(0.5\ \mathrm{K})^2$ along the diagonal. The values of the cost function for different continuum scaling factor combinations are shown in Fig. 8(b). It is clear that the SGP MWR data set places much tighter constraints on the continuum values than the COPS MWRHF data set. However, the results are consistent with those at 31.4 GHz for the assumption of no bias offset for either the MWR or MWRHF data.

The 150-GHz region shows negligible sensitivity to errors in the water vapor line parameters. Aside from the uncertainties associated with the scatter on the model/measurement comparisons, the largest additional uncertainties are those in the bias offsets for the MWR and the MWRHF. Turner *et al.* [34], in their analysis of the 150-GHz data from the COPS, had inferred that a bias offset of 0.49 K was necessary for the MWR 23.8-GHz channel. Applying such an offset has an impact on the retrieved PWV scaling factors and, hence, on the continuum values derived from the 150-GHz data. The application of an offset is the main reason for the difference in their derived continuum scaling factors from ours, although their factors, $0.835\ +/-0.07$ (foreign) and $1.44\ +/-0.31$ (self), are in agreement with those in this paper within the stated error bars. The error bounds provided in this paper are tighter due to the large PWV range of the 31.4-GHz data set.

C. *Continuum Validation at 170* GHz

The GVRP, also known as the MP183, was built by Radiometrics and has over 1000 tunable channels. For the measurements used in this paper, fifteen channels from 170 to 183.31 GHz were calibrated for use. The GVRP bandwidth is determined by an eight-pole intermediate frequency (IF) filter, characterized by sharp cutoffs. The 3-dB bandwidth IF bandpass filter is nominally 25–500 MHz, although the actual measured bandwidth is slightly wider. Thus, the effective RF bandwidth is 1118 MHz with a 30-MHz notch in the middle and is virtually identical for all channels. Concerning the GVRP calibration, noise diode injection is used to measure the system gain continuously. The receiver temperature is measured once per observation cycle using an internal blackbody target. The noise diode effective temperature is calibrated once every few months using an external liquid nitrogen target, leading to an estimated accuracy of $\sim$1 K, depending on the channel [11].

The GVRP data set used for this paper is from a deployment of the instrument at the ARM SGP site from January to March 2008. The instrument had previously been deployed alongside two other 183-GHz radiometers at the ARM North Slope of Alaska site for measurements of extremely low water vapor conditions during the RHUBC during February and March 2007 [11], [12], [34], but since the RHUBC was conducted during extremely dry atmospheric conditions, the RHUBC GVRP data set is of limited use for water vapor continuum model validation. However, the RHUBC comparisons between

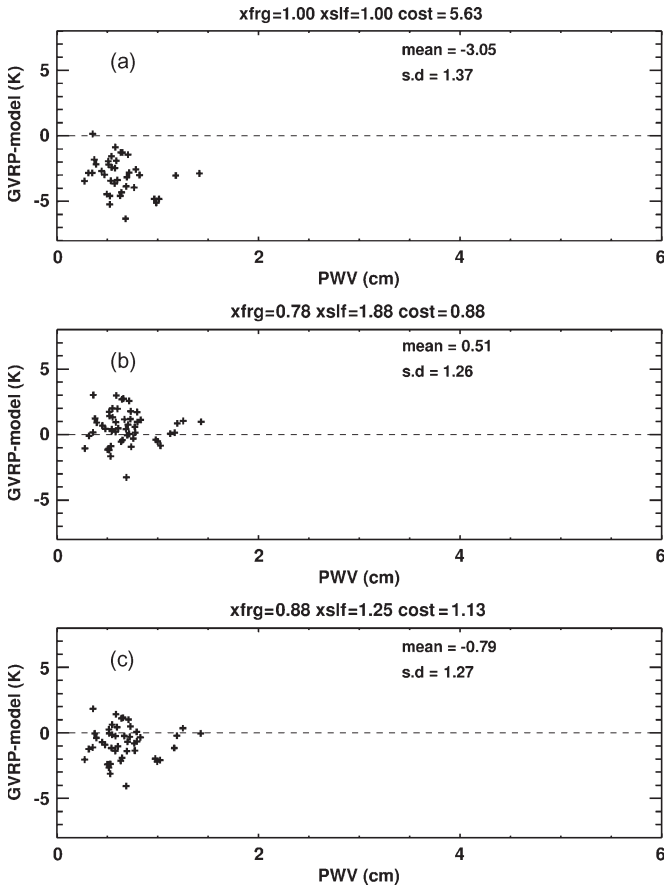

Fig. 10. Residuals at 170 GHz, after the scaling of PWV using the 23.8-GHz MWR channel for (a) MT_CKD 2.1, (b) "Rosenkranz-like" continuum values, and (c) proposed values for MT_CKD 2.4.

the three independent 183-GHz instruments have provided a high degree of confidence in the GVRP calibration.

The deployment of the GVRP at the SGP site resulted in 77 clear-sky radiosonde matches, with PWV values ranging from 0.27 to 2.1 cm. As with the 31.4-GHz and 150-GHz data sets presented in the previous sections, the GVRP data were averaged over a 35-min time period around the sonde launch. Clear-sky cases were determined using a combination of the test on the standard deviation of the 31.4-GHz channel of the colocated MWR over the sonde launch time window and data from a ceilometer. Fig. 5(e) and (f) shows the "raw" model/measurement comparisons for the MWR 23.8-GHz channel and for the GVRP 170-GHz channel. Again, the large negative bias in the 170-GHz residuals in Fig. 5(f) is partly due to the radiosonde bias as discussed in Section IV-A and partly due to the continuum errors in MT_CKD v2.1, which result in larger brightness temperature residuals at this higher frequency than at 31.4 GHz.

Again, scaling factors for the radiosonde PWV were retrieved using the 23.8-GHz MWR channel. No instrument offsets were applied to the 23.8-GHz channel before the PWV retrievals. Fig. 10 shows the 170-GHz model/measurement comparisons resulting from the scaled radiosonde profiles for different continuum scaling factors. The cost function J_2, with a measurement covariance matrix with $(1\ \mathrm{K})^2$ along the diagonal, was used to assess the quality of the residuals. Fig. 8(c) shows a 2-D representation of the cost function surface. Fig. 8(a)–(c) shows a high degree of consistency between the continuum adjustment factors that would be determined from each of the three independent data sets.

V. Discussion

Fig. 11 shows the modeled brightness temperature spectra and model/model differences relative to MonoRTM v4.2 (which uses MT_CKD 2.4; see Table I) for four different standard atmospheres: subarctic winter (0.94-cm PWV), U.S. standard (1.4-cm PWV), midlatitude summer (2.9-cm PWV), and tropical (4.0-cm PWV). The shapes of the differences vary with the PWV due to the interplay between the changes in the foreign- and self-broadened water vapor continua (which dominate at low and high PWV, respectively). Note that the model simulations in Fig. 11 include only water vapor, oxygen, and nitrogen in the modeled spectra. It can be seen that, despite the limited number of molecules included in the simulations, there are some sharper features in the MonoRTM/Rosenkranz differences. These are due to the differences in the number of oxygen (sharp differences around the 60-GHz band) and water vapor lines included in the two models. For the drier atmospheres shown (subarctic winter and U.S. standard), the update in the continuum from MT_CKD 2.1 (used in MonoRTM v4.0) to MT_CKD 2.4 (used in MonoRTM v4.2) brings the MonoRTM results somewhat closer to the Rosenkranz model results than they were before.

Fig. 12 (top) shows the impact of the MT_CKD continuum update on the retrievals of PWV at 23.8 GHz, for both the upwelling and downwelling measurements. The effect of the update is an increase in inferred PWV for a given atmosphere, and the impact is largest for the lowest water vapor cases (1.4% at 0.3-cm PWV, decreasing to 1% at 1.5 cm). The magnitude of the effect on the PWV retrievals is not large since the absorption at 23.8 GHz is dominated by the line rather than the continuum absorption. Moreover, shown in Fig. 12 (bottom) is the impact on the PWV retrievals of a 0.5-K bias offset assumption for the 23.8-GHz channel for a ground-based retrieval. For low water vapor conditions, the effect of the bias offset is far larger than the effect of the continuum change.

Fig. 13 shows the sensitivity of the retrievals of the LWP to the MT_CKD v2.1 to MT_CKD v2.4 continuum update for varying water vapor conditions, for both the upwelling and downwelling measurements. Sensitivity tests were performed both assuming fixed PWV and for the case where the PWV was adjusted to take account of the impact of the continuum change on the retrieval (see Fig. 12). Only points for which the frequencies are not saturated with respect to water vapor have been plotted. (Higher frequencies for the upwelling case are saturated, plus the higher frequencies are not normally used in operational cloud water retrievals due to the higher uncertainties associated with surface emissivity.) These results are based on LWP less than 200 $\mathrm{g \cdot m^{-2}}$ so are applicable to thinner clouds. For thicker clouds, the results would be less sensitive to changes in the water vapor continuum. At lower frequencies, the results are similar for upwelling and downwelling radiation.

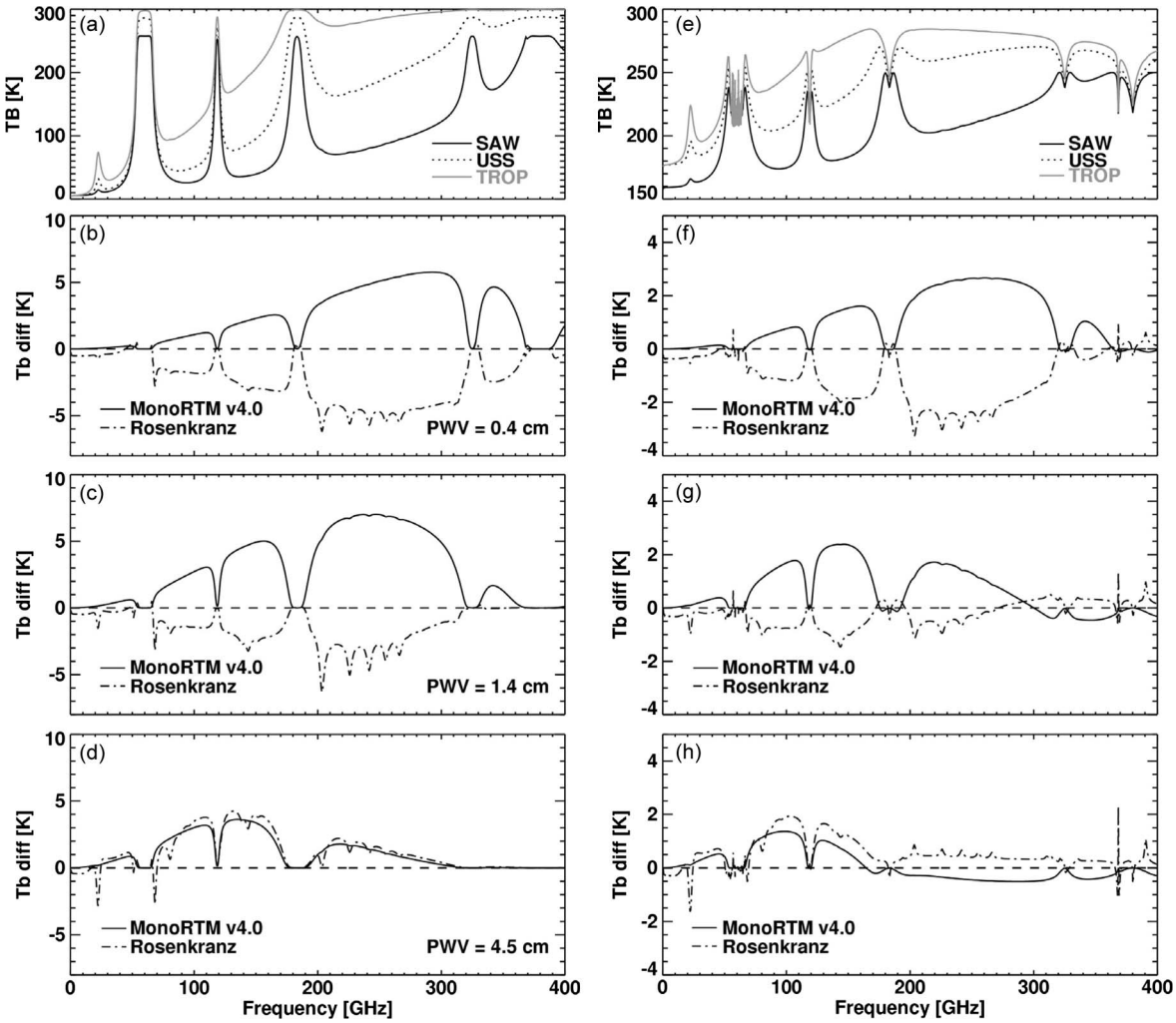

Fig. 11. Modeled brightness temperatures and model/model difference spectra for a range of standard atmospheres: subarctic winter, U.S. standard, and tropical. (a)–(d) Left column shows the spectra and differences for the downwelling (ground-based) view. (e)–(h) Right column shows the spectra and differences for an upwelling (space-based) view. All upwelling calculations used a surface emissivity of 0.6. Surface temperatures were 260 K for the subarctic winter case and 290 K for the U.S. standard and tropical cases.

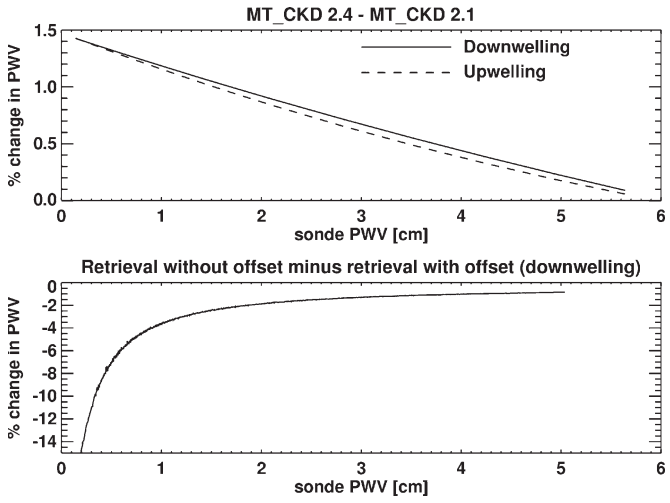

Fig. 12. (Top) Difference in inferred PWV (from retrieval at 23.8 GHz) resulting from the continuum update. (Bottom) Difference in retrieved PWV (from 23.8 GHz) arising from the assumption of no instrument bias offset versus a 0.5-K offset. Sensitivity calculations were based on a U.S. Standard Atmosphere with scaled column water vapor, a surface temperature of 290 K, and a surface emissivity of 0.6.

The water vapor continuum update presented here also could have potential implications for the determination of sea surface emissivity from space. The effect of the continuum update is the decrease in the modeled brightness temperature for a given scene, which, if all other parameters were to stay the same, would imply a decrease in surface emissivity. In theory, this could have implications for ocean surface wind speed retrievals, but in practice, intelligent ocean wind retrieval algorithms use optimized channel configurations that minimize sensitivity to the atmosphere, so the effect of a change in the continuum model is likely mitigated to some extent.

The ARM ground-based radiometer measurements are extremely valuable for the validation of spectroscopy in the context of radiative transfer modeling. Improvements in these models can have a positive impact on weather prediction, either through the assimilation of the retrieved atmospheric and surface parameters discussed earlier or through the direct assimilation of radiances. In addition, since MWRs are often used to obtain reference estimates of water vapor from the ground, improvements in microwave spectroscopy used in the models can also result in improvements of the knowledge of

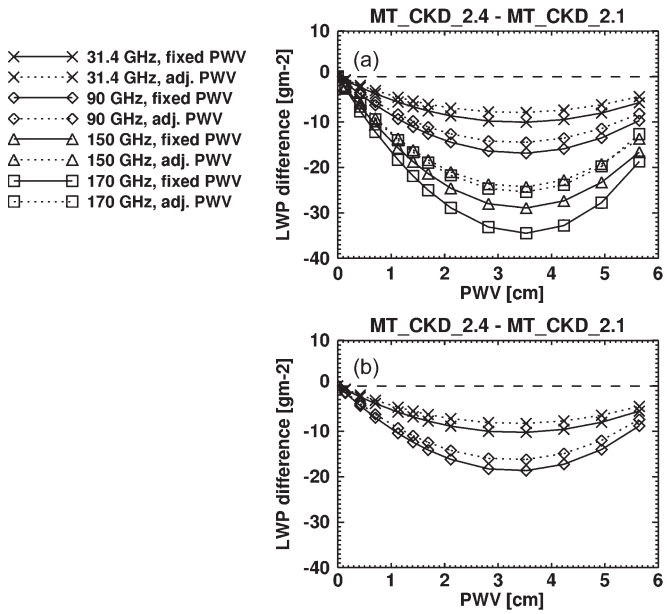

Fig. 13. Difference in inferred LWP (from retrievals at different window frequencies) resulting from the continuum update. The upper plot is for the downwelling case, while the lower plot is for the upwelling case. Solid lines show the difference in inferred LWP, assuming that the retrieved PWV remains fixed in spite of the continuum change. Dotted lines show the difference in inferred LWP, accounting for the adjustment in the retrieved PWV caused by the continuum change. Sensitivities are based on LWP less than 200 $g \cdot m^{-2}$. Only frequencies that do not become saturated with respect to water vapor have been plotted. (Higher frequencies for the upwelling case can be saturated.) Sensitivity calculations were based on a U.S. Standard Atmosphere with scaled column water vapor, a surface temperature of 290 K, and a surface emissivity of 0.6.

the spectroscopy in other spectral regions, with further implications for weather and/or climate prediction. For example, Delamere *et al.* [12] have used microwave water vapor measurements to aid in improvements to the water vapor continuum in the far IR, a spectral region of crucial importance in the calculation of atmospheric cooling rates [4].

VI. Conclusion

With the recent advances in the accuracy of fast radiative transfer models relative to line-by-line models, the limiting factor on the accuracy of the modeling of gaseous absorption using radiative transfer models is our knowledge of the spectroscopy (line parameters, line shape, and continuum). High-quality radiometric measurements, in conjunction with the *in situ* measurements of the atmospheric state, are extremely valuable for spectroscopy validation in the context of atmospheric remote sensing. The validation of spectroscopy against ground-based measurements avoids any uncertainties associated with the modeling of surface parameters that are inherent in the model/measurement comparisons of upwelling radiation, offers opportunities for a range of coincident measurements for the characterization of the atmospheric state, provides the advantage of better temporal and spatial colocation with *in situ* profile measurements (from radiosondes), and minimizes issues of representativeness.

In this paper, updates have been made to both the MT_CKD self- and foreign-broadened water vapor continuum absorption (used in MonoRTM) in the microwave region. The updates were based on comparisons between the MonoRTM and a range of ground-based radiometer measurements at 31.4 and 170 GHz made at the ARM SGP site in Oklahoma as well as the 150-GHz measurements from the COPS campaign in the Black Forest, Germany. While the tightest constraints on the continuum absorption were provided by the 31.4-GHz data set, since this data set provided the largest number of measurements over the widest range of water vapor conditions (see Table II), results indicate good consistency between the different instruments and frequencies analyzed. The high quality of the calibration of each of the three instruments used was the key to this paper. The uncertainty on the new foreign-broadened water vapor continuum in MT_CKD 2.4 is estimated at 4% and the uncertainty on the self-broadened water vapor continuum is also estimated at 4%.

In the future, it would be desirable to have data sets that would also validate the continuum at the higher 150- and 170-GHz frequencies over a wide range of PWV values and that would provide enough information to allow the validation of the temperature dependence of the continuum.

The updates implemented in the MT_CKD v2.4 continuum resulted not only from this paper but also from the work using ground-based spectrally resolved measurements in the far IR by Delamere *et al.* [12]. Measurements at wavelengths between the microwave and far-IR regions could provide further confidence in the water vapor continuum model in both regions and in the consistency across this entire spectral range. For most locations on the Earth, the region between the microwave and the far IR is opaque, so measurements from the ground offer information on the near-surface temperature rather than on RT model parameters. However, measurements in this region have been made in extremely dry conditions from a site in the Atacama Desert, Chile, during the RHUBC-II in August to October 2009 [34]. The analysis of these measurements is underway.

Acknowledgment

The authors would like to thank S. A. Clough of Clough Radiation Associates for initiating our work on microwave continuum validation using ARM data, for his input to this analysis, for building the continuum that links these microwave updates smoothly to the updates by Delamere *et al.* in the far IR, and for input on earlier versions of the manuscript. The authors would also like to thank M. Cadeddu for information on the ARM radiometers and their calibration and D. Turner for sharing his careful screening of the COPS data set for clouds and dew. The authors would like to thank T. Meissner for providing information on the RSS work that went into the empirical adjustment of the Rosenkranz continuum for AMSR retrievals and S. Boukabara for all his work on the early development and testing of MonoRTM.

References

[1] D. E. Burch, *Continuum Absorption by H2O*, 1981, AFGL-TR-81-0300.
[2] S. A. Clough, F. X. Kneizys, R. W. Davies, R. Gamache, and R. H. Tipping, "Theoretical line shape for H2O vapor: Application to the continuum," in *Atmospheric Water Vapor*, A. Deepak, T. D. Wilkerson, and L. H. Ruhnke, Eds. London, U.K.: Academic, 1980, pp. 25–46.

[3] S. A. Clough, F. X. Kneizys, and R. W. Davies, "Line shape and the water vapor continuum," *Atmos. Res.*, vol. 23, pp. 229–241, Jun. 1989.
[4] S. A. Clough, M. J. Iacono, and J.-L. Moncet, "Line-by-line calculation of atmospheric fluxes and cooling rates: Application to water vapor," *J. Geophys. Res.*, vol. 97, no. D14, pp. 15761–15785, Oct. 1992.
[5] S. A. Clough and K. E. Cady-Pereira, "The physical retrieval of PWV and CLW with MonoRTM using ARM MWR data," in *Proc. 12th Atmos. Radiat. Meas. Sci. Team Meeting*, St. Petersburg, FL, Apr. 2002.
[6] S. A. Clough, M. W. Shephard, E. Mlawer, J. S. Delamere, M. Iacono, K. E. Cady-Pereira, S. Boukabara, and P. D. Brown, "Atmospheric radiative transfer modeling: A summary of the AER codes," *J. Quant. Spectrosc. Radiat. Transf.*, vol. 91, no. 2, pp. 233–244, Mar. 2005.
[7] S. A. Clough, Y. Beers, J. P. Klein, and L. S. Rothman, "Dipole moment of water from Stark measurements of H2O, HDO and D2O," *J. Chem. Phys.*, vol. 59, pp. 2254–2259, Sep. 1973.
[8] M. P. Cadeddu, V. H. Payne, S. A. Clough, K. E. Cady-Pereira, and J. C. Liljegren, "Effect of the oxygen line parameter modeling on temperature and humidity retrievals from ground-based microwave radiometers," *IEEE Trans. Geosci. Remote Sens.*, vol. 45, no. 7, pp. 2216–2223, Jul. 2007.
[9] M. P. Cadeddu, J. C. Liljegren, and A. Pazmany, "Measurements and retrievals from a new 183-GHz water vapor radiometer in the Arctic," *IEEE Trans. Geosci. Remote Sens.*, vol. 45, no. 7, pp. 2207–2215, Jul. 2007.
[10] K. E. Cady-Pereira, M. W. Shephard, D. D. Turner, E. J. Mlawer, and S. A. Clough, "Improved total column PWV from Vaisala RS90 and RS92 humidity sensors," *J. Atmos. Ocean. Technol.*, vol. 25, no. 6, pp. 873–883, Jun. 2008.
[11] D. Cimini, F. Nasir, E. R. Westwater, V. H. Payne, D. D. Turner, E. J. Mlawer, M. Exner, and M. P. Cadeddu, "Comparison of ground-based millimeter-wave observations and simulations in the Arctic winter," *IEEE Trans. Geosci. Remote Sens.*, vol. 47, no. 9, pp. 3098–3106, Sep. 2009.
[12] J. S. Delamere, S. A. Clough, V. H. Payne, E. J. Mlawer, D. D. Turner, and R. R. Gamache, "A far-IR radiative closure study in the Arctic: Application to water vapor," *J. Geophys. Res.*, vol. 115, p. D17106, 2010.
[13] Y. Han and E. R. Westwater, "Analysis and improvement of tipping calibration for ground-based microwave radiometers," *IEEE Trans. Geosci. Remote Sens.*, vol. 38, no. 3, pp. 1260–1276, May 2000.
[14] T. J. Hewison, D. Cimini, L. Martin, C. Gaffard, and J. Nash, "Validating clear air absorption models using ground-based microwave radiometers and vice-versa," *Meteorol. Zeitschrift*, vol. 15, no. 1, pp. 27–36, Feb. 2006. doi:10.1127/09412948/2006/0097.
[15] M. A. Koshelev, M. Y. Tretyakov, G. Y. Golubiatnikov, V. V. Parshin, V. N. Markov, and I. A. Koval, "Broadening and shifting of the 321, 325 and 380 GHz lines of water vapor by pressure of atmospheric gases," *J. Mol. Spectrosc.*, vol. 241, no. 1, pp. 101–108, Jan. 2007.
[16] H. J. Liebe, G. A. Hufford, and M. G. Cotton, "Propagation modeling of moist air and suspended water/ice particles below 1000 GHz," in *Proc. Advis. Group Aerosp. Res. Dev. (AGARD) 52nd Special Meeting Panel Electromagn. Wave Propag.*, Palma de Mallorca, Spain, May 17–21, 1993, pp. 3-1–3-10.
[17] H. J. Liebe and D. H. Layton, "Millimeter-wave properties of the atmosphere: Laboratory studies and propagation modeling," F Natl. Telecomm. Inf. Admin., Boulder, CO, NTIA Report 87-224, 1987.
[18] H. J. Liebe and T. A. Dillon, "Accurate foreign-gas broadening parameters of the 22-GHz H2O line from refraction spectroscopy," *J. Chem. Phys.*, vol. 50, pp. 727–732, 1969.
[19] J. C. Liljegren, "Automatic self-calibration of ARM microwave radiometers," in *Microwave Radiometry and Remote Sensing of the Earth's Surface and Atmosphere*, P. Pampaloni and S. Paloscia, Eds. Zeist, The Netherlands: VSP Press, 2000, pp. 433–443.
[20] B. Lin, P. Minnis, A. Fan, J. A. Curry, and H. Gerber, "Comparison of cloud liquid water paths derived from *in situ* and microwave radiometer data taken during the SHEBA/FIREACE," *Geophys. Res. Lett.*, vol. 28, no. 6, pp. 975–978, Mar. 2001.
[21] C. Lucas and E. J. Zipser, "Environmental variability during TOGA-COARE," *J. Atmos. Sci.*, vol. 57, no. 15, pp. 2333–2350, Aug. 2000.
[22] R. Marchand, T. Ackerman, E. R. Westwater, S. A. Clough, K. Cady-Pereira, and J. C. Liljegren, "An assessment of microwave absorption models and retrievals of cloud liquid water using clear-sky data," *J. Geophys. Res.*, vol. 108, no. D24, p. 4773, Dec. 2003. doi:10.1029/2003JD003843.
[23] T. Meissner, private communication, 2000.
[24] C. Melsheimer, C. Verdes, S. A. Buehler, C. Emde, P. Eriksson, D. G. Feist, S. Ichizawa, V. O. John, Y. Kasai, G. Kopp, N. Koulev, T. Kuhn, O. Lemke, S. Ochiai, F. Schreier, T. R. Sreerkha, M. Suzuki, C. Takahashi, S. Tsujimaru, and J. Urban, "Intercomparison of general purpose clear sky atmospheric radiative transfer models for the millimeter/submillimeter spectral range," *Radio Sci.*, vol. 40, p. RS1007, 2005. doi:1029d2004RS0031109.
[25] L. M. Miloshevich, H. Vömel, D. N. Whiteman, B. M. Lesht, F. J. Schmidlin, and F. Russo, "Absolute accuracy of water vapor measurements from six operational radiosonde types launched during AWEX-G and implications for AIRS validation," *J. Geophys. Res.*, vol. 111, no. D09, p. D09 S10, Apr. 2006.
[26] V. H. Payne, J. S. Delamere, K. E. Cady-Pereira, R. R. Gamache, J.-L. Moncet, E. J. Mlawer, and S. A. Clough, "Air-broadened half-widths of the 22 and 183 GHz water vapor lines," *IEEE Trans. Geosci. Remote Sens.*, vol. 46, no. 11, pp. 3601–3617, Nov. 2008.
[27] A. L. Pazmany, "An operational G-band (183 GHz) water vapor radiometer," *IEEE Trans. Geosci. Remote Sens.*, vol. 45, no. 7, pp. 2202–2206, Sep. 2007.
[28] W. H. Press, B. P. Flannery, S. A. Teulosky, and W. T. Vetterling, *Numerical Recipes in C: The Art of Scientific Computing*, 2nd ed. Cambridge, U.K.: Cambridge Univ. Press, 1992.
[29] P. W. Rosenkranz, "Water vapor microwave continuum absorption: A comparison of measurements and models," *Radio Sci.*, vol. 33, no. 4, pp. 919–928, Jul. 1998.
[30] P. W. Rosenkranz and C. D. Barnet, "Microwave radiative transfer model validation," *J. Geophys. Res.*, vol. 111, no. D9, p. D09S07, Mar. 2006.
[31] C. Serio, F. Esposito, G. Masiello, G. Pavese, M. R. Calvello, G. Grieco, V. Cuomo, H. L. Buijs, and C. B. Roy, "Interferometer for ground-based observations of emitted spectral radiance from the troposphere: Evaluation and retrieval performance," *Appl. Opt.*, vol. 47, no. 21, pp. 3909–3919, Jul. 2008. doi:10.1364/AO.47.003909.
[32] M. W. Shephard, S. A. Clough, V. H. Payne, W. L. Smith, S. Kireev, and K. E. Cady-Pereira, "Performance of the line-by-line radiative transfer model (LBLRTM) for temperature and species retrievals: IASI case studies from JAIVEx," *Atmos. Chem. Phys.*, vol. 9, pp. 7397–7417, Oct. 2009.
[33] M. Y. Tretyakov, M. A. Koshelev, V. V. Dorovskikh, D. S. Makarov, and P. W. Rosenkranz, "60-GHz oxygen band: Precise broadening and central frequencies of fine-structure lines, absolute absorption profile at atmospheric pressure, and revision of mixing-coefficients," *J. Mol. Spectrosc.*, vol. 231, no. 1, pp. 1–14, May 2005.
[34] D. D. Turner and E. J. Mlawer, "Radiative heating in underexplored bands campaigns (RHUBC)," *Bull. Amer. Meteorol. Soc.*, vol. 91, no. 7, pp. 911–923, Jul. 2010.
[35] D. D. Turner, B. M. Lesht, S. A. Clough, J. C. Liljegren, H. E. Revercomb, and D. C. Tobin, "Dry bias and variability RS80-H radiosondes: The ARM experience," *J. Atmos. Ocean. Technol.*, vol. 20, no. 1, pp. 117–132, Jan. 2003.
[36] D. D. Turner, A. M. Vogelmann, R. T. Austinm, J. C. Barnard, K. E. Cady-Pereira, J. C. Chiu, S. A. Clough, C. Flynn, M. M. Khaiyer, J. Liljegren, K. Johnson, B. Lin, C. Long, A. Marshak, S. Y. Matrosov, S. A. MacFarlane, M. Miller, Q. Min, P. Minnis, W. O'Hirok, Z. Wang, and W. Wiscombe, "Thin liquid water clouds: Their importance and our challenge," *Bull. Amer. Meteorol. Soc.*, vol. 88, no. 2, pp. 177–190, Feb. 2007.
[37] D. D. Turner, S. A. Clough, J. C. Liljegren, E. E. Clothiaux, K. Cady-Pereira, and K. L. Gaustad, "Retrieving liquid water path and precipitable water vapor from Atmospheric Radiation Measurement (ARM) microwave radiometers," *IEEE Trans. Geosci. Remote Sens.*, vol. 45, no. 11, pp. 3680–3690, Nov. 2007. doi:10.1109/TGRS.2007.903703.
[38] D. D. Turner, U. Loehnert, M. Cadeddu, S. Crewell, and A. Vogelmann, "Modifications to the water vapor continuum in the microwave suggested by ground-based 150 GHz observations," *IEEE Trans. Geosci. Remote Sens.*, vol. 47, no. 10, pp. 3326–3337, Oct. 2009.
[39] J. H. Van Vleck and D. L. Huber, "Absorption, emission and linebreadths: A semihistorical perspective," *Rev. Mod. Phys.*, vol. 49, no. 4, pp. 939–959.
[40] H. Vömel, H. Selkirk, L. Miloshevich, J. Valverde, J. Valdés, E. Kyrö, R. Kivi, W. Stolz, G. Peng, and J. A. Diaz, "Radiation dry bias of the Vaisala RS92 humidity sensor," *J. Atmos. Ocean. Technol.*, vol. 24, no. 6, pp. 653–863, Jun. 2007.
[41] F. J. Wentz and T. Meissner, *AMSR Ocean Algorithm Theoretical Basis Document*, ver. 2, Remote Sens. Syst., Santa Rosa, CA, private communication, 2000.
[42] F. J. Wentz, "A well calibrated ocean algorithm for special sensor microwave/imager," *J. Geophys. Res.*, vol. 102, no. C4, pp. 8703–8718, Apr. 1997.
[43] P. Zuidema, E. R. Westwater, C. Fairall, and D. Hazen, "Ship-based liquid water path estimates in marine stratocumulus," *J. Geophys. Res.*, vol. 110, no. D20, p. D20206, 2005. doi:10.1029/2005JD005833.

Vivienne H. Payne received the M.Phys. degree in physics from the University of Edinburgh, Edinburgh, U.K., in 2001, and the D.Phil. degree in atmospheric physics from the University of Oxford, Oxford, U.K.

She is currently a Staff Scientist with the Atmospheric Composition and Radiation Section, Atmospheric and Environmental Research, Inc., Lexington, MA. She is a member of the National Aeronautics and Space Administration Science Teams for the Tropospheric Emission Spectrometer on the Aura satellite and for the Global Precipitation Measurement mission. Her principal areas of interest include the retrieval and scientific utilization of information from remotely sensed measurements, atmospheric radiative transfer in the microwave and infrared regions, and molecular spectroscopy in the context of atmospheric remote sensing.

Eli J. Mlawer received the B.A. degree in mathematics and astronomy from Williams College, Williamstown, MA, in 1982, the B.A. and M.A. degrees in physics from Cambridge University, Cambridge, U.K., in 1984 and 1990, respectively, and the Ph.D. degree in physics from Brandeis University, Waltham, MA, in 1994.

Since then, he has been with Atmospheric and Environmental Research, Inc., Lexington, MA, where he is the Leader of the Atmospheric Composition and Radiation Section. He is the Coleader of the Continual Intercomparison of Radiation Codes effort to evaluate the quality of radiation codes used in climate simulations. He was the Coprincipal Investigator of the two Radiative Heating in Underexplored Bands Campaigns, field experiments that took place in northern Alaska (2007) and Chile (2009) directed at increasing our understanding of radiative processes in the far-infrared spectral region of importance to climate. He is the developer of the MT_CKD water vapor continuum model, a key component in the majority of existing atmospheric radiative transfer models. His research interests include atmospheric radiative transfer and climate. He has primary responsibility for the design, implementation, and validation of RRTM, a radiative transfer model for climate applications used by many climate and weather prediction models.

Karen E. Cady-Pereira received the B.S. degree in physics from the University of Sao Paulo, Sao Paulo, Brazil, in 1980, and the M.S. degree in oceanography from the Massachusetts Institute of Technology, Cambridge, in 1984.

For 18 years, she has been with Atmospheric and Environmental Research, Inc., Lexington, MA, where she, at first, was with the General Circulation group and, since 1994, has been with the Remote Sensing and Radiation and Climate groups. She has worked on a wide range of radiative transfer problems, from determining bidirectional reflectance distribution function from multiangle imaging spectroradiometer measurements to measuring atmospheric water vapor using microwave radiometers and, most recently, on developing retrieval algorithms for trace gases from Tropospheric Emission Spectrometer measurements. She is particularly interested in the scattering from surfaces (such as icy planets, vegetated land, and sea surface) and from particles in the atmosphere.

Jean-Luc Moncet received the B.Eng. degree in applied physics from the Ecole Nationale Superieure de Physique, Marseilles, France, in 1981, the M.Sc. degree in telecommunications from the Institut National de la Recherche Scientifique, Quebec City, QC, Canada, in 1984, and the M.Sc. degree in meteorology from McGill University, Montreal, QC, in 1989.

He has been the Head of the Remote Sensing Division with Atmospheric and Environmental Research (AER), Inc., Lexington, MA, which oversees the activities of the Infrared, Microwave, Trace Gases, and Cloud Remote Sensing groups. During his accumulated 20 years of experience in infrared, microwave, and ultraviolet remote sensing and radiative transfer modeling, he has led the environmental data record (EDR) algorithm development effort for both the infrared and microwave instruments on the National Polar-orbiting Operational Environmental Satellite System and has served as the Principal Investigator in several other government-funded research programs. He is the codeveloper of the unified retrieval concept, now used in the Cross-track Microwave Scanner, Advanced Microwave Sounding Unit, Cross-track Infrared Sounder, and Ozone Mapping and Profiler Suite EDR algorithms, and has participated in the Special Sensor Microwave Temperature-2 and Special Sensor Microwave Image/Sounder calibration/validation effort. Since joining AER, he has developed high-speed high spectral resolution radiative transfer algorithms (including the optimal spectral sampling method [US Patent] and the Code for High-Resolution Atmospheric Radiative Transfer with Scattering for monochromatic radiance calculations in scattering atmospheres) and inversion algorithms for application to spaceborne infrared down-looking and limb sensors and airborne and ground-based interferometers. He has also provided support to the aerospace industry for several instrument trade studies. He is a member of the National Aeronautics and Space Administration Advanced Microwave Scanning Radiometer and Atmospheric Infrared Sounder science teams. His other areas of activity include cloud property retrievals from infrared spectrometric measurements and combined microwave/electro-optical imagers, numerical weather prediction model assimilation, and radiation/climate studies.